AGU PUBLICATIONS

JGR

Journal of Geophysical Research: Space Physics

RESEARCH ARTICLE

10.1002/2015JA022266

Key Points:

- Radiation from IB processes are measured in VLF magnetic fields up to 2630 km away
- LOREs are strongly associated with lightning exhibiting intense IB and fast first leaders
- Observed properties of LORE causative discharges do not signify association with any particular TLE

Correspondence to:
D. A. Kotovsky,
dakotovsky@ufl.edu

Citation:
Kotovsky, D. A., et al. (2016), Initial breakdown and fast leaders in lightning discharges producing long-lasting disturbances of the lower ionosphere, *J. Geophys. Res. Space Physics*, *121*, 5794–5804, doi:10.1002/2015JA022266.

Received 11 DEC 2015
Accepted 24 MAY 2016
Accepted article online 29 MAY 2016
Published online 28 JUN 2016

Initial breakdown and fast leaders in lightning discharges producing long-lasting disturbances of the lower ionosphere

D. A. Kotovsky[1], R. C. Moore[1], Y. Zhu[1], M. D. Tran[1], V. A. Rakov[1], J. T. Pilkey[1], J. A. Caicedo[1], B. Hare[1], D. M. Jordan[1], and M. A. Uman[1]

[1] Department of Electrical and Computer Engineering, University of Florida, Gainesville, Florida, USA

Abstract The recent discovery of long recovery, early VLF scattering events (LOREs) indicates that the electric field changes from lightning discharges are capable of producing long-lasting disturbances (up to tens of minutes) in the upper mesosphere and lower ionosphere. Comparison of lightning mapping array, broadband (up to 10 MHz) electric field, and VLF (~300 Hz to 42 kHz) magnetic field measurements shows that the field changes produced by initial breakdown (IB) processes and the following leaders in natural, cloud-to-ground lightning discharges are detectable in VLF magnetic field measurements at long distances. IB radiation has been detected in VLF for lightning discharges occurring up to 2630 km away from the VLF observing station. Radio atmospherics associated with 52 LOREs, 51 regular recovery events, and 3098 flashes detected by National Lightning Detection Network and/or GLD360 were examined for IB radiation occurring up to 15 ms before the return stroke. Our analysis reveals that in contrast to regular recovery early VLF events, LOREs are strongly associated with lightning discharges which exhibit an intense IB process and a fast first leader (typical duration <4 ms). These experimental results demonstrate that initial breakdown and leader processes are indicators of discharge properties highly relevant to the total energy transfer between lightning discharges and the middle/upper atmosphere.

1. Introduction

Early VLF scattering events manifest as the perturbations of subionospherically propagating VLF transmissions that occur within 20 ms of a lightning discharge [*Inan et al.*, 1993], indicating that the lightning discharge has a direct effect on the overlying ionosphere. *Cotts and Inan* [2007] have recently identified a new class of long recovery, early events (LOREs) which can exhibit recovery times up to tens of minutes, much greater than typical early event recovery times of 60–240 s (1–4 min) [*Sampath et al.*, 2000]. The observations of LOREs demonstrate the capability of lightning discharges to produce long-lasting effects on the middle and upper atmosphere.

Chemical mechanisms explaining both typical and long recoveries of VLF scattering events have been modeled by *Kotovsky and Moore* [2016]. According to their work, long recovery VLF scattering events result from large electron density enhancements whose loss is controlled by slow electron-ion recombination processes, occurring when attachment rates are small and/or when detachment rates balance out attachment rates. The large electron density enhancements necessary to produce long recovery VLF scattering require that a significant amount of energy be deposited into the lower ionosphere by the causative lightning discharge.

Recent statistical studies of LOREs have identified a number of important lightning discharge properties that are associated with LOREs. *Haldoupis et al.* [2013] and *Salut et al.* [2013] report that both the probability of detecting an early VLF event and the expected event recovery duration increase with lightning peak current inferred from lightning locating systems. A large number of LOREs have been associated with lightning flashes occurring over oceans [e.g., *Cotts and Inan*, 2007; *Salut et al.*, 2012], which may in part be due to the higher occurrence of oceanic, negative flashes with large inferred peak currents [*Said et al.*, 2013] and large inferred charge moment changes [*Füllekrug et al.*, 2002].

LOREs are associated with both positive (+) and negative (−) cloud-to-ground flashes (CGs) [*Haldoupis et al.*, 2013; *Salut et al.*, 2013]. *Haldoupis et al.* [2013] observed 340 LOREs (>300 s recovery) produced by lightning discharges with peak currents greater than 200 kA and reported that 110 were associated with −CGs, and

230 were associated with +CGs. Conducting a smaller study, *Salut et al.* [2013] report that for 90 early VLF events with estimated recoveries > 200 s, 20 were associated with −CGs and 70 were associated with +CGs. For comparison with typical recovery events, *Salut et al.* [2013] report that for 1160 early VLF events with estimated recoveries < 200 s, 276 were associated with −CGs and 924 were associated with +CGs (i.e., a similar proportion of −CGs producing typical recovery and producing long recovery events).

The association of LOREs with both positive and negative polarity flashes, in addition to the observations of large elves and elve-sprite pairs in association with LOREs reported by *Haldoupis et al.* [2012], led *Haldoupis et al.* [2013] to conclude that LOREs were produced by ionospheric conductivity changes associated with elves, due to the polarity-invariant theory of elve production by the lightning electromagnetic pulse [e.g., *Barrington-Leigh and Inan*, 1999; *Newsome and Inan*, 2010]. Their argument, however, disregards evidence that −CGs account for nearly half, if not more, of all sprite halos [e.g., *Newsome and Inan*, 2010; *Williams et al.*, 2012] and that rare circumstances of "negative" sprites have been observed [e.g., *Barrington-Leigh et al.*, 1999; *Taylor et al.*, 2008; *Li et al.*, 2012]. Additionally, gigantic jets are capable of effective upward transport of either negative or positive charge [*van der Velde et al.*, 2010]. Consequently, the association of LOREs with both positive and negative polarity discharges does not designate or preclude the involvement of any specific transient luminous event.

In this paper, we report on the relationship between recoveries of early VLF events and the initial breakdown process of the causative lightning discharges. Initial breakdown (IB) or preliminary breakdown (PB) refers to in-cloud processes at the beginning of lightning flashes which produce electromagnetic radiation in the form of characteristic pulses [e.g., *Clarence and Malan*, 1957; *Weidman and Krider*, 1979; *Beasley et al.*, 1982]. IB pulses have been observed in both −CGs [e.g., *Clarence and Malan*, 1957; *Marshall et al.*, 2014; *Zhu et al.*, 2015] and +CGs [e.g., *Ushio et al.*, 1998; *Nag and Rakov*, 2012; *Wu et al.*, 2013]. Recent statistical analyses by *Stolzenburg et al.* [2013] and *Marshall et al.* [2014] suggest that all CG and intracloud flashes begin with an IB process. For detailed information regarding the physical nature of IB, we refer the reader to the recent experimental works of *Campos and Saba* [2013], *Stolzenburg et al.* [2013, 2014], and *Wilkes et al.* [2016]. Recent efforts in modeling currents in initial breakdown processes include the works of *Karunarathne et al.* [2014], *da Silva and Pasko* [2015], and *Nag and Rakov* [2016].

We identify that long-lasting disturbances of the lower ionosphere are strongly associated with lightning discharges which exhibit an intense IB process and fast leaders (durations <4 ms) which precede first return strokes of both positive and negative polarity flashes. Consequently, the thundercloud charge and electric field configurations which result in an intense IB process and fast first leaders are highly relevant to the coupling of lightning energy to the middle and upper atmosphere. In section 2, we summarize more recent reports regarding the relationships among IB and other lightning discharge properties. In section 3, the instrumentation and methodology utilized in this work are discussed. In section 4, we show simultaneous measurements of IB pulses using lightning mapping array, broadband electric field, and VLF magnetic field data. Also in section 4, we present a statistical analysis of IB radiation detected in VLF radio atmospherics associated with 52 LOREs, 51 regular recovery early VLF events, and 3098 flashes detected by National Lightning Detection Network (NLDN) and/or GLD360. Lastly, in section 5, the implications of our observations are summarized.

2. Initial Breakdown and Other Discharge Properties

Within the current literature, there are conflicting reports regarding the relationships between the intensity of the IB process and the speeds of the following leaders [*Brook*, 1992; *Nag and Rakov*, 2009; *Wu et al.*, 2013; *Marshall et al.*, 2014; *Zhu et al.*, 2015], and between leader speeds and peak currents of the following return stroke [*Idone et al.*, 1984; *Jordan et al.*, 1992; *Campos et al.*, 2014; *Zhu et al.*, 2015]. More expansive studies may be required in order to sort out the apparent discrepancies. Regardless of what these relationships happen to be, our observations indicate that the relationships among IB processes, leader processes, and other discharge properties are pertinent to the production of long-lasting ionospheric disturbances.

Nag and Rakov [2009] proposed a theory regarding the influence of the thundercloud lower positive charge region (LPCR) on the propagation of negative leaders in lightning discharges. In their framework, it is assumed that IB pulses in −CGs are produced as a negative leader descends through the LPCR. Principally, the LPCR increases the electric field between the main negative charge region and the LPCR (where breakdown occurs) and reduces the electric field below the LPCR. As a result, LPCRs may act to enhance the intensity of the IB process (or the initial leader process) but inhibit the propagation of the leader below the LPCR (if the LPCR is not consumed during the IB process or as the negative leader traverses the LPCR). When the LPCR region is large, IB may be intense but leader speeds may be relatively slow. When the LPCR is small or negligible, IB may be very weak but leader speeds may be fast. Leader speeds might also be affected by any removal of the LPCR during IB.

Brook [1992] suggested that intense IB and fast stepped leaders observed for discharges in winter thunderstorms over Albany, NY, were indicative of higher electric fields initiating those discharges. Consequently, *Brook* [1992] concluded that discharges exhibiting intense IB and fast leaders may be more energetic. We note that intense IB and fast first leaders have been observed for discharges in summer thunderstorms [e.g., *Heavner et al.*, 2002; *Marshall et al.*, 2014; *Kolmašová et al.*, 2014; *Zhu et al.*, 2015] as well as in winter thunderstorms [e.g., *Brook*, 1992; *Wu et al.*, 2013]. In the context of the *Nag and Rakov* [2009] theory, scenarios of intense IB and fast first leaders might result if significant portions of the local LPCR are removed during the IB process or as the leader propagates through the LPCR.

Wu et al. [2013] observed that measured ratios of IB and return stroke field intensity (IB-RS ratio) were inversely correlated to measured time delays between IB and the following return stroke (IB-RS interval). Measured IB-RS intervals indicate the maximum leader duration, as leaders can initiate either during or immediately following the IB stage [*Stolzenburg et al.*, 2014]. *Marshall et al.* [2014] observed a similar correlation between the range-normalized intensities of IB pulses and IB-RS intervals. On the other hand, *Zhu et al.* [2015] reported no clear trend between IB-RS ratios and IB-RS intervals measured for 214 −CGs.

Zhu et al. [2015] identified a strong inverse correlation between IB-RS intervals of −CGs (i.e., maximum stepped leader durations) and first return stroke peak currents for 222 flashes. As well, speeds of negative dart leaders in natural and triggered lightning have been observed to be correlated with peak currents of the following return stroke [*Idone et al.*, 1984; *Jordan et al.*, 1992]. On the other hand, *Campos et al.* [2014] reported no observed correlation between leader speeds and return stroke peak currents for negative stepped leaders, negative dart leaders, or positive leaders.

Association between flashes exhibiting high average leader speeds and the occurrence of elves has been reported by *Frey et al.* [2005]. In their work, the IB process was inferred from the detection of initial brightening in photometric channels and VLF radiation occurring prior to first return strokes. Of the 593 elves observed, 294 were associated with lightning exhibiting short IB-RS intervals (∼3 to 4 ms), indicating that the lightning leaders exhibited fast average speeds (on the order of 10^6 m s^{-1} or greater). *Frey et al.* [2005] suggested that if faster stepped leaders are capable of more efficient ionization of the lightning channel [e.g., *Idone et al.*, 1984], the subsequent return stroke would produce more electromagnetic radiation capable of more efficient elve production.

We note that *Frey et al.* [2005] compared their observed leader speeds only to the reported speeds of the "α-type" and "β-type" portions of stepped leaders [*Schonland*, 1937; *Schonland et al.*, 1938a, 1938b]. Citing the apparent continuous propagation of positive leaders in photographic and video observations [e.g., *Berger and Vogelsanger*, 1966; *Saba et al.*, 2008], *Frey et al.* [2005] consequently restricted themselves to concluding that the observed, fast leader speeds were associated only with −CGs. However, positive leaders can also exhibit fast average speeds (> 10^6 m s^{-1}), as demonstrated by the optical studies of *Berger and Vogelsanger* [1966] [see *Saba et al.*, 2008] and *Campos et al.* [2014]. Additionally, short IB-RS intervals measured for 15 +CGs (polarity reported by NLDN) presented in this work seem to further demonstrate the capability of positive leaders to exhibit fast average speeds.

3. Description of the Experiment

The observations reported in this paper are recorded by the following instruments: a multistation VHF lightning mapping array (LMA), operated at the University of Florida (UF) International Center for Lightning Research and Testing (ICLRT, 29.94°N, 82.03°W); a broadband electric field antenna, operated at the UF Lightning Observatory in Gainesville (LOG, 29.63°N, 82.33°W); and three magnetic VLF loop antennas, of the UF Ionospheric Radio Laboratory (locations detailed below).

The LMA operated at the ICLRT is a network of eight VHF receiver stations utilized to identify and locate sources of RF radiation (66–72 MHz) associated with breakdown processes in lightning discharges. Each LMA station records the time and amplitude of the largest RF pulse detected every 10 μs with ∼40 ns timing accuracy.

Time-of-arrival analysis is then applied to the data collected from all LMA stations to identify the location, magnitude, and time of RF emission sources. Further details about the ICLRT's LMA operation and methodology can be found in *Pilkey* [2014] and *Pilkey et al.* [2014].

The electric field system operated at LOG is an elevated circular flat-plate antenna installed on the roof of a five-story building, with an integrating amplifier. The system has a decay time constant of 10 ms, and an upper cutoff frequency of 10 MHz. Electric field measurements are recorded with 8 bit resolution at a sampling rate of 100 MHz. For more details about the instrumentation at LOG [see *Rakov et al.*, 2014; *Zhu et al.*, 2015, and references therein].

The three VLF antenna receivers are operated at Melbourne, Florida (MB, 28.06°N, 80.62°W); Tuscaloosa, Alabama (NS, 33.47°N, 87.63°W); and San Antonio, Texas (SA, 29.76°N, 98.57°W). The effective bandwidth of the VLF systems is from ~300 Hz to ~42 kHz. Signals broadcasted by VLF transmitters NAA (24.0 kHz, Cutler, Maine), NLM (25.2 kHz, LaMoure, North Dakota), and NAU (40.75 kHz, Aguanda, Puerto Rico) are processed and recorded with both 20 ms and 1 s resolution, while accurate timing provided by a GPS-trained oscillator with 10^{-12} frequency precision. The receivers at NS and SA employ two orthogonal loop antennas, directed geomagnetically north-south and east-west, while the MB receiver operates one loop directed to maximize the signal from NLM. Further details regarding the VLF receivers and methodology can be found in *Mitchell* [2015].

A perturbation of a VLF transmission is identified as an "early" event by the detection of a radio atmospheric (spheric) occurring less than 20 ms before the event onset. Scattered fields are calculated from the observed amplitude and phase perturbations using the method of *Dowden et al.* [1997]. Events having a scattered field magnitude lasting >300 s are considered long recovery. Fifty-two LOREs and fifty-one regular recovery early events are analyzed in this work. Data from the National Lightning Detection Network (NLDN) [*Orville*, 1991] and Global GLD360 [*Said et al.*, 2010] are used to identify lightning flash location, polarity, and peak current, when possible.

Comparison of electric field and VLF measurements of IB pulses has provided the criteria for identifying electromagnetic radiation from the IB process in VLF data in cases where no accompanying high-time resolution electric or magnetic field measurements are available. All event causative spherics are analyzed for "initial breakdown candidate" radiation (>8 dB signal-to-noise ratio) occurring within 15 ms before the main spheric front produced by the return stroke. Candidates which cannot be unambiguously distinguished from activities of unrelated flashes are categorized as "indeterminate cases." For all but 12 events (1 LORE and 11 typical recovery), the event causative spherics are taken to be produced by first return strokes, either through the detection of initial breakdown and/or by the absence of other CG spherics within 300 ms before the event causative spheric. For the remaining 12 events, we are unable to determine if the event causative spherics were produced by first return strokes or subsequent return strokes.

Additionally, spherics for 3092 NLDN detected flashes (having occurred in 10 s time segments encompassing observed early VLF events) are examined for detection of IB radiation. In addition to the 3092 NLDN detected flashes, we analyze 6 event causative flashes that were detected only by GLD360; as such, 3098 lightning location system (LLS) detected flashes are analyzed. Other GLD360 detected flashes were not analyzed, to avoid possible double counting with NLDN detected flashes.

Among all lightning flashes, IB pulses were rarely observed in VLF (with > 8 dB SNR) at distances greater than a few hundred kilometers, as will be discussed in the next section. Based on this criterion, we have classified the IB radiation reported in this paper (observed at distances greater than a few hundred kilometers) as "intense." Recent experimental and modeling studies indicate that peak currents producing IB pulses may be as large as several tens of kiloamps [*Karunarathne et al.*, 2014; *da Silva and Pasko*, 2015; *Kolmašová et al.*, 2016], flowing over channels with lengths on the order of a few hundred meters to a kilometer [*Stolzenburg et al.*, 2013, 2014; *Karunarathne et al.*, 2014; *da Silva and Pasko*, 2015; *Nag and Rakov*, 2016]. Such large currents have been demonstrated to produce initial breakdown observable at a distance of 600 km [*Kolmašová et al.*, 2014, 2016]. In this work, IB radiation was observed up to distances of ~2630 km.

4. Experimental Observations

Simultaneous LMA, broadband electric field, and VLF magnetic field observations of a natural, −CG first return stroke exhibiting large IB pulses is presented in Figure 1. Distances to the NLDN-inferred ground strike location

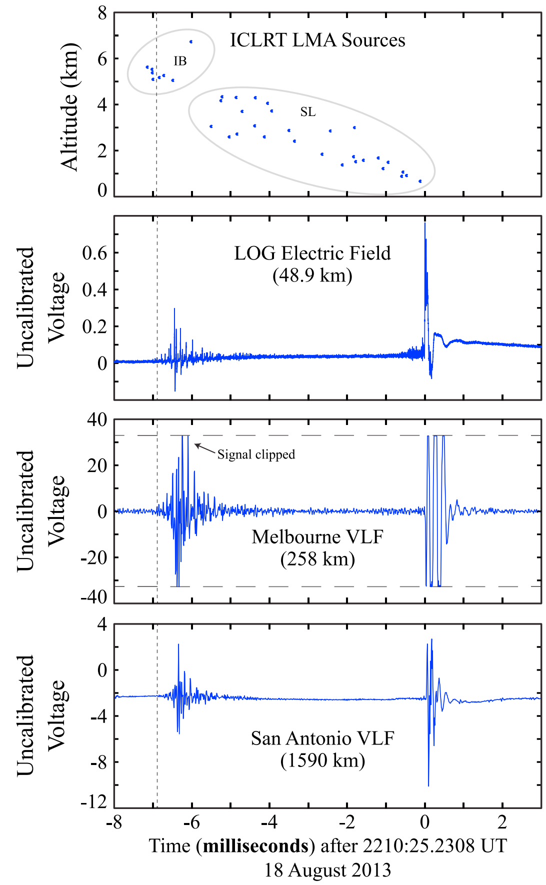

Figure 1. (first panel) Correlated LMA, (second panel) electric field, and (third and fourth panels) VLF data. Initial breakdown (IB) pulses preceding a fast stepped leader (SL) are observed in both electric field and VLF data, with a waveform comparable to those observed in the majority of LORE-associated spherics. Note that the LOG wideband electric field and VLF magnetic field systems employ different electronic amplification gains and exhibit different uncalibrated output scales and saturation levels.

are shown, and propagation delays were removed in the shown data (assuming speed of light propagation). The LMA sources were calculated using 6 and 7 station solutions, limited to chi-square values of 6 or less when assuming a 70 ns timing error.

LMA sources shown in Figure 1 (first panel) indicate the descent of LMA sources during the IB process (possibly an initial leader) [*Stolzenburg et al.*, 2014] and during the stepped leader (SL) process. The LMA sources associated with the IB stage at the start of the flash occur at altitudes between 5 and 6 km, consistent with the inferred altitudes of the bottom of negative charge regions in typical north Florida thunderstorms [*Pilkey et al.*, 2014]. The IB pulses are evident in the electric fields measured at LOG ~48.9 km from the lightning discharge. The return stroke initiated approximately 6.8 ms following the start of IB. Given that the IB initiated above 5 km, the average leader speed was greater than $\sim 7 \times 10^5$ m s^{-1}. Radiation from both the IB stage and the return stroke were measured by the VLF receivers at Melbourne (~258 km) and San Antonio (~1590 km). Note that LOG wideband electric field system was designed to measure large fields of nearby flashes, whereas the VLF systems were designed to measure small fields from distant lightning. As a result, the LOG and VLF systems employ different electronic amplification gains and exhibit different uncalibrated output scales and saturation levels. Individual IB pulses cannot be fully resolved in VLF due to the limited time resolution of the VLF systems (10 μs).

IB pulses of 10 −CGs (IB-RS <15 ms) were simultaneously measured by the LOG electric field antenna and VLF receivers. Comparisons of these measurements allow for the discrimination of radiation from the IB process in VLF observations where no accompanying high-time resolution electric or magnetic field data are available. Additionally, these observations seem to confirm that the "initial brightening" and VLF radiation observed by

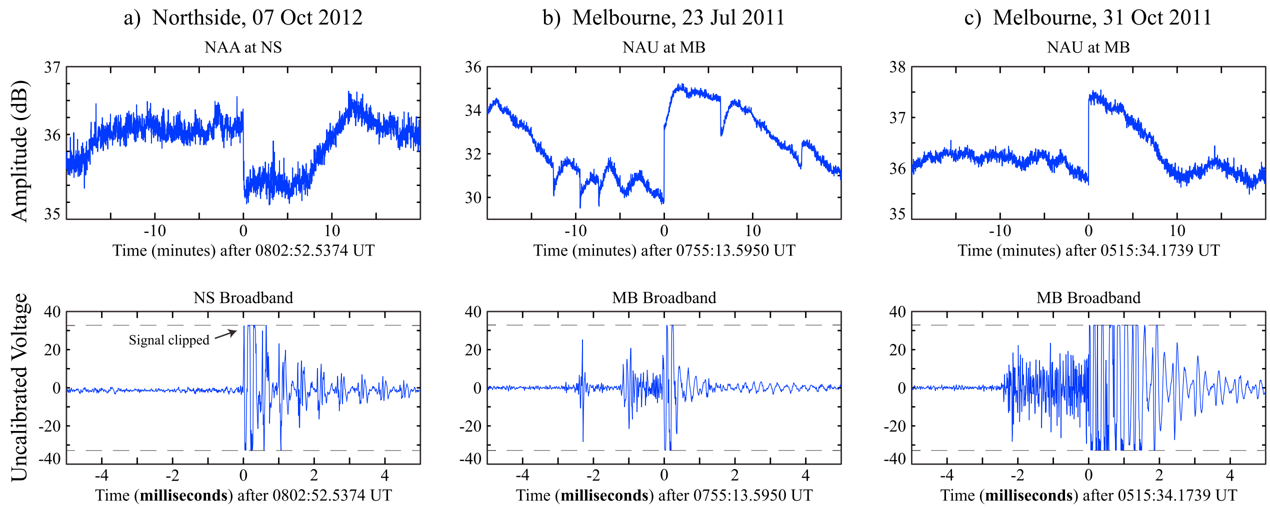

Figure 2. Three examples of (top row) long recovery, early VLF events and (bottom row) associated spherics. Note the different timescales between figures on the top and bottom rows. Signal clipping level is shown with dashed grey lines. (a) A typical spheric (without detected initial breakdown radiation) is exhibited; (b) initial breakdown radiation detected with a quiet interval; (c) initial breakdown detected without a quiet interval.

Frey et al. [2005] were in fact observations of breakdown processes. We note that *Frey et al.* [2005] did not have high-time resolution electric or magnetic field measurements capable of definitively distinguishing IB pulses.

Spherics associated with early VLF scattering events were examined for IB radiation occurring within 15 ms before the main spheric front. Figures 2a–2c show examples of LOREs (top row) and their associated spherics (bottom row)—note the difference in timescales between figures on the top row and the figures on the bottom row. A typical spheric waveform is shown in Figure 2a, exhibiting a sharp rise followed by damped oscillations associated with the propagation of the return stroke radiation field within the Earth-ionosphere waveguide (i.e., direct wave plus ionospheric and ground reflections). In this and many other spheric waveforms, no lightning-related radiation is detectable prior to the return stroke field change. However, some spheric waveforms (e.g., Figures 2b, 2c, and 1) exhibit IB radiation just prior to (typically <4 ms), and in most cases leading up to the main spheric front. Spherics are observed both with (e.g., Figures 2b and 1) and without (e.g., Figure 2c) a quiet interval at some point between the start of IB radiation and the return stroke field change. In some cases (e.g., Figure 1), the quiet intervals observed in distant VLF measurements might relate to "intermediate stages" sometimes observed in measurements of relatively close lightning discharges (some hundreds of kilometers or less) [e.g., *Clarence and Malan*, 1957; *Beasley et al.*, 1982]. In other cases (e.g., Figure 2c), the quiet intervals observed in distant VLF measurements might relate to quiet intervals between multiple IB pulse trains we sometimes observe in LOG electric field measurements of relatively close lightning discharges. Note, however, that analysis of lightning waveforms observed at long distances (e.g., hundreds of kilometers and beyond) may be significantly complicated by the effects of propagation in the Earth-ionosphere waveguide.

Occurrence statistics of detected IB radiation were compared among spherics of 52 long recovery early events, 51 regular recovery early events, and 3098 LLS detected flashes. Figure 3 (right column) displays the location maps for the event causative discharges (top), and for all LLS detected discharges with clearly identifiable spherics (bottom). Circles denote spherics associated with long recovery events, and crosses denote spherics associated with regular recovery events. Red colored markers indicate that IB radiation was detected, black colored markers indicate that IB radiation was not detected, and green colored markers indicate that the detection of IB radiation was "indeterminate." Twenty-eight of 52 LOREs occurred over predominantly ocean propagation paths, and 13 of 29 LLS detected flashes associated with LOREs located over ocean.

Ten LOREs exhibited wide scattering angles between 15° and 40° (assuming disturbances are centered above causative discharges). Additionally, two LORE causative spherics were time correlated with NLDN detected flashes that would lead to exceptionally wide angle scattering (∼92°) in one case, and backscatter (∼176°) in the other case. From the available data, we are unable to independently determine if these two NLDN detected flashes are the LORE causative flashes.

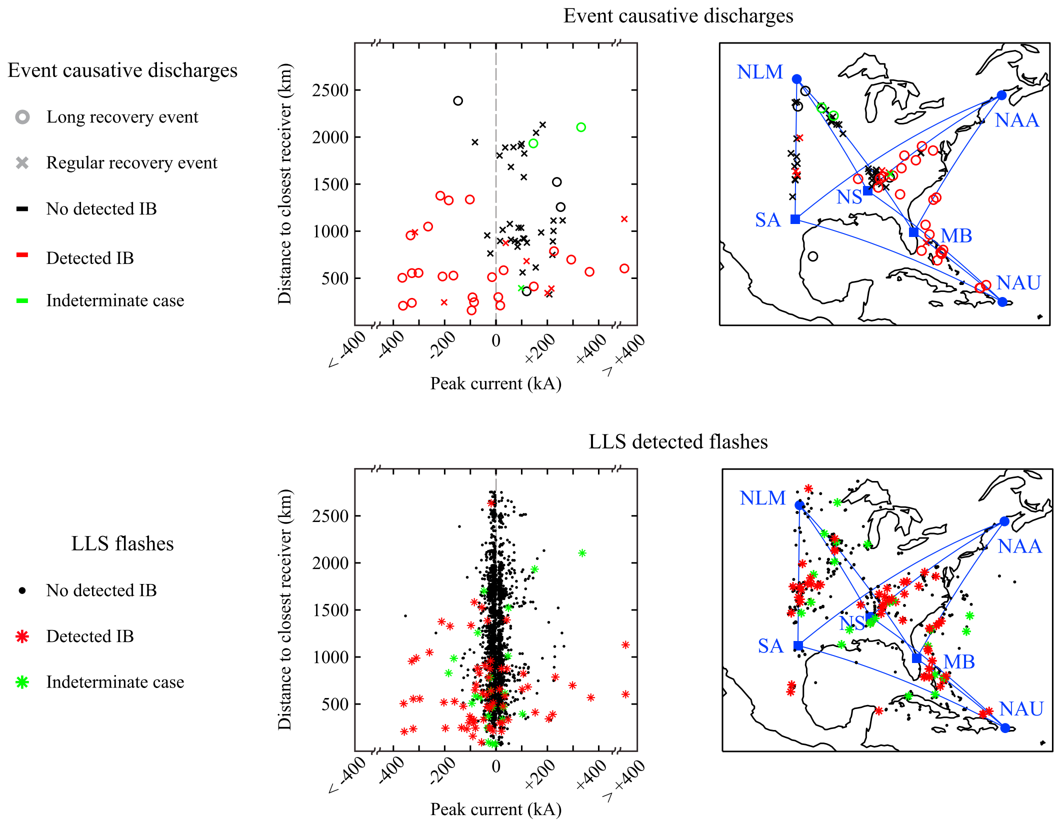

Figure 3. (right column) Maps of transmitter and receiver geometry, with LLS detected flashes, and (left column) peak current and distance relationships for (top row) early VLF event causative flashes, and (bottom row) all LLS detected flashes. The map of LLS discharges (Figure 3, bottom right) include only discharges with clearly identifiable spherics. Circles (crosses) indicate causative flashes of long (regular) recovery events. Red, black, and green markers indicate that initial breakdown radiation was detected, not detected, or possible/indeterminate, respectively.

Figure 3 (left column) shows scatterplots of the inferred peak current and measurement distance for event causative discharges (top row) and all LLS detected discharges analyzed (bottom row). As compared to regular recovery causative discharges, a significant portion of LORE causative discharges are negative polarity (see Table 1). We note that 11 of the 13 oceanic LORE causative discharges were negative polarity.

IB radiation was definitively detected up to a distance of 2630 km, and up to 1375 km for early VLF event causative discharges. We note that IB pulses have been detected by broadband (few hundred hertz to 5 MHz) electric field measurements up to distances of ~600 km [*Kolmašová et al.*, 2014, 2016], and radiation from the IB process has been inferred in ELF/VLF (50 Hz to 30 kHz) magnetic field measurements to distances of at least ~2200 km [*Frey et al.*, 2005]. Our observations seem to confirm the inferences of *Frey et al.* [2005].

Table 1. Observed Initial Breakdown Statistics for all VLF events and LLS Detected Flashes[a]

	# of Spherics: For All VLF Events and LLS Flashes								
	LOREs			Typical Recovery			LLS Flashes		
	IB Detected	No IB Detected	Indeterminate Case	IB Detected	No IB Detected	Indeterminate Case	IB Detected	No IB Detected	Indeterminate Case
Positive flash	8	3	2	5	31	1	21	1285	8
Negative flash	16	1	0	2	3	0	48	1721	15
No LLS data	16	5	1	1	7	1	-	-	-
Total	40	9	3	8	41	2	69	3006	23

[a]Statistics shown for all LORE events, all typical recovery events, and all LLS detected flashes. Polarity of flashes are taken as reported from NLDN or GLD360.

Table 2. Observed Initial Breakdown Statistics for a Restricted Set of VLF Events and LLS Detected Flashes[a]

	# of Spherics: Peak Current > 50 kA, Within 1500 km of RX								
	LOREs			Typical Recovery			LLS Flashes		
	IB Detected	No IB Detected	Indeterminate Case	IB Detected	No IB Detected	Indeterminate Case	IB Detected	No IB Detected	Indeterminate Case
Positive flash	5	2	0	4	19	1	11	51	1
Negative flash	15	0	0	2	0	0	31	57	6
Total	20	2	0	6	19	1	42	108	7

[a] Statistics shown only for discharges with a peak current greater than 50 kA occurring within 1500 km of the observing receiver. Polarity of flashes are taken as reported from NLDN or GLD360.

Table 1 shows the statistics regarding the number of spherics detected: (a) with IB radiation, (b) without IB radiation, or (c) with indeterminate or possible IB radiation. Note that LLS detected spherics producing VLF events are counted in the statistics for both "LLS flashes" and their respective VLF event (either "LORE" or "typical recovery"). A large proportion of LORE causative discharges exhibited detectable IB (77% of 52 events). In contrast, the proportion for discharges exhibiting detectable IB was much smaller for both typical recovery events (16% of 51 events) and LLS detected flashes (2% of 3098 flashes).

In Table 2, spheric statistics are shown only for LLS detected flashes with large peak currents (>50 kA) that occurred within 1500 km of the observing receiver. This range was selected, informed by the results of Figure 3, in order to (1) exclude small flashes whose IB might not be detectable except at very close distances and (2) exclude flashes at large distances where the IB radiation is too greatly attenuated. For this restricted subset of spheric statistics, the proportion of LORE causative discharges exhibiting detectable IB remains large (91% of 22 events). In contrast, the proportion of discharges with detectable IB is still much smaller for both typical recovery events (23% of 26 events) and LLS detected flashes (27% of 157 flashes).

For the 40 LORE-producing discharges with detected IB radiation (occurring within 15 ms before the return stroke), the IB-RS intervals (in this paper, measured from the start of the IB radiation to the start of the RS field change) ranged from 1.0 to 12.6 ms, with a mean value of 3.5 ms and a median value of 2.4 ms. In the cases where the IB-RS intervals were exceptionally short (e.g., <2 ms), it is possible that the measured VLF radiation was produced by leader processes not occurring during the IB stage. The measured IB-RS intervals indicate the maximum duration of the leader process, as leaders can initiate either during or immediately following the IB stage [*Stolzenburg et al.*, 2014]. For a leader path length that is less than 7 km, the mean IB-RS interval of 3.5 ms results in an average leader speed $\geq 2 \times 10^6$ m s^{-1}, and the median IB-RS interval of 2.4 ms results in an average leader speed $\geq 3 \times 10^6$ m s^{-1} (consistent with speeds of initial leaders or the "β-type" portion of leaders [*Stolzenburg et al.*, 2014; *Schonland*, 1938a, 1938b]). In contrast, typical average speeds of both negative and positive polarity leaders range from 1×10^5 to 5×10^5 m s^{-1} [*Rakov and Uman*, 2003; *Saba et al.*, 2008] (consistent with speeds of the "α-type" portion of leaders [*Schonland*, 1937; *Schonland et al.*, 1938a, 1938b]).

Fifteen NLDN detected flashes classified as +CGs exhibited detectable IB radiation in the VLF measurements, and 10 were associated with observed early VLF events (6 LOREs and 4 regular recovery). The measured IB-RS intervals for these 15 +CGs range from 0.5 ms to 10.7 ms, with a mean value of 2.9 ms and a median value of 1.7 ms. The short IB-RS intervals indicate that the positive leaders in these discharges were likely fast. For 11 of the 15 +CGs, the measured IB-RS intervals were shorter than <2 ms, and it is possible that the measured radiation for these 11 events were produced by leader processes not occurring during the IB stage.

5. Discussion

Simultaneous LMA, electric field, and VLF observations have been utilized to classify detection of radiation from the IB process in VLF measurements, and IB radiation was detected in VLF for lightning discharges at distances up to 2630 km away from the observing receiver (up to 1375 km for discharges producing observable VLF scattering events). Consequently, the use of VLF receivers can greatly support the study of initial breakdown and its significance on other lightning discharge properties. The definitive observations of the IB process in VLF measurements at long distances support the inference of *Frey et al.* [2005] that the optical and VLF observations reported therein are measurements of IB radiation.

The association of LOREs with both positive and negative polarity flashes, a significant occurrence rate of LORE causative flashes over oceans, and the observation of LOREs at wide scattering angles are in agreement with past observations [*Cotts and Inan*, 2007; *Salut et al.*, 2012, 2013; *Haldoupis et al.*, 2012, 2013]. For the 30 LOREs with associated LLS data, 13 were associated with positive lightning flashes and 17 were associated with negative lightning flashes (see Table 1). Note that the relatively high percentage of LOREs produced by negative flashes reported in this study (57% of 30 events) — as compared to those reported by *Haldoupis et al.* [2013] (32% of 340 events) and *Salut et al.* [2013] (22% of 90 events) — may likely be due to our limited number of LORE observations with associated LLS data.

Given that elves, sprite halos, sprites, and gigantic jets can each be associated with both positive and negative discharges, the results of this study do not indicate that LOREs are associated with only one particular kind of transient luminous event. This is contrary to the conclusions of *Haldoupis et al.* [2013], who argue that LOREs are distinctly associated with elves.

Long-lasting (>300 s) disturbances of the lower ionosphere produced by lightning discharges are strongly associated with discharges exhibiting an intense IB process and fast first leaders of both positive and negative flashes. The short IB-RS intervals (typically less than 4 ms) in LORE causative lightning indicate average leader speeds ($\geq 10^6$ m s^{-1} for channel lengths $\geq$4 km). In contrast, there appears to be no special relationship between typical recovery VLF events and lightning exhibiting intense IB radiation and fast first leaders. We note that although nearly all LOREs were associated with lightning exhibiting intense IB radiation and fast first leaders, these source properties are alone not sufficient conditions to produce LOREs.

The modeling work of *Kotovsky and Moore* [2016] suggests that a large energy input into the lower ionosphere is required for the production of LOREs. At this time, it is unclear which lightning properties (including those of IB and RS processes) are directly responsible for producing the long-lasting ionospheric disturbances. While it has been shown by *Haldoupis et al.* [2013] and *Salut et al.* [2013] that the expected event recovery increases with return stroke peak current, a causal physical relationship has not yet been determined. Note that our observations of intense initial breakdown in discharges producing LOREs do not necessarily indicate the involvement of high peak currents and large electromagnetic pulse radiation in producing the long-lasting ionospheric disturbance. A number of different and possibly related discharge properties (e.g., return stroke speed, peak current, charge moment change, and spectral content) may act in concert to generate the large electric field changes (including quasi-electrostatic, induction, and radiation components) necessary to produce long-lasting ionospheric disturbances.

Further, there is still uncertainty regarding the detailed physical relationships between (1) thundercloud charge structure and initial breakdown, (2) initial breakdown intensity and leader speeds, (3) leader speeds and return stroke currents, and (4) return stroke currents and the electric field changes that produce ionospheric disturbances. Consequently, we cannot determine at this time if the occurrence of intense initial breakdown is causally linked with, for example, higher return stroke electromagnetic pulse radiation or larger quasi-electrostatic field changes. Regardless, the results presented in this paper demonstrate that there is a statistically significant relationship between LOREs and the detection of initial breakdown and fast leaders in the causative lightning discharge. In contrast, this statistical relationship does not hold for typical recovery ionospheric disturbances.

In conclusion, our results demonstrate that the thundercloud charge and electric field configurations which lead to an intense IB process and fast first leaders are highly relevent to the properties of lightning discharges which produce long-lasting ionospheric disturbances. Consequently, understanding the physical mechanisms involved in breakdown and leader processes is important for investigating the total energy transfer between lightning discharges and the middle/upper atmosphere.

Acknowledgments
This work is supported by DARPA/US Air Force contract FA8650-15-C-7535 and NSF grants PLR-1246275 and AGS-1521747 to the University of Florida. We would like to thank Vaisala for generously providing lightning data from the NLDN and GLD360 data set. Data utilized in this paper are available upon request by contacting R.C. Moore (moore@ece.ufl.edu).

References

Barrington-Leigh, C. P., and U. S. Inan (1999), Elves triggered by positive and negative lightning discharges, *Geophys. Res. Lett.*, *26*(6), 683–686.

Barrington-Leigh, C. P., U. S. Inan, M. Stanley, and S. A. Cummer (1999), Sprites triggered by negative lightning discharges, *Geophys. Res. Lett.*, *26*(24), 3605–3608.

Beasley, W., M. A. Uman, and P. L. Rustan Jr. (1982), Electric fields preceding cloud-to-ground lightning flashes, *J. Geophy. Res.*, *87*(C7), 4883–4902.

Berger, K., and E. Vogelsanger (1966), Photographische Blitzuntersuchungen der Jahre 1955–1965 auf dem Monte San Salvatore, *Bull. Schweiz. Elektrotech. Ver.*, *57*, 599–602.

Boeck, W. L., O. H. Vaughan Jr., R. Blakeslee, B. Vonnegut, and M. Brook (1992), Lightning induced brightening in the airglow layer, *Geophys. Res. Lett.*, *19*(2), 99–102.

Brook, M. (1992), Breakdown electric fields in winter storms, *Res. Lett. Atmos. Electr.*, *12*, 47–52.

Campos, L. Z. S., and M. M. F. Saba (2013), Visible channel development during the initial breakdown of a natural negative cloud-to-ground flash, *Geophys. Res. Lett.*, *40*, 4756–4761.

Campos, L. Z. S., M. M. F. Saba, T. A. Warner, O. Pinto Jr., E. P. Krider, and R. E. Orville (2014), High-speed video observations of natural cloud-to-ground lightning leaders—A statistical analysis, *Atmos. Res.*, *135–136*, 285–305.

Clarence, N. D., and D. J. Malan (1957), Preliminary discharge processes in lighting flashes to ground, *Q. J. R. Meteorol. Soc.*, *83*, 161–172.

Cotts, B. R. T., and U. S. Inan (2007), VLF observation of long ionospheric recovery events, *Geophys. Res. Lett.*, *34*, L14809, doi:10.1029/2007GL030094.

da Silva, C. L., and V. P. Pasko (2015), Physical mechanism of initial breakdown pulses and narrow bipolar events in lightning discharges, *J. Geophys. Res. Atmos.*, *120*, 4989–5009, doi:10.1002/2015JD023209.

Dowden, R. L., J. B. Brundell, and C. J. Rodger (1997), Temporal evolution of very strong Trimpis observed at Darwin, Australia, *Geophys. Res. Lett.*, *24*(19), 2419–2422.

Haldoupis, C., M. Cohen, B. Cotts, E. Arnone, and U. Inan (2012), Long-lasting *D* region ionospheric modifications, caused by intense lightning in association with elve and sprite pairs, *Geophys. Res. Lett.*, *39*(L16801), doi:10.1029/2012GL052765.

Haldoupis, C., M. Cohen, E. Arnone, B. Cotts, and S. Dietrich (2013), The VLF fingerprint of elves: Step-like and long recovery Early VLF perturbations caused by EM pulses radiated by powerful ± CG lightning, *J. Geophys. Res. Space Physics*, *188*(118), 5392–5402, doi:10.1002/jgra.50489.

Frey, H. U. et al. (2005), Beta-type stepped leader of elve-producing lightning, *Geophys. Res. Lett.*, *32*, L13824.

Füllekrug, M., C. Price, Y. Yair, and E. R. Williams (2002), Intense ocean lightning, *Ann. Geophys.*, *20*, 133–137.

Heavner, M. J., D. A. Smith, A. R. Jacobson, and R. J. Sheldon (2002), LF/VLF and VHF lightning fast-stepped leader observations, *J. Geophys. Res.*, *107*(D24), 4791, doi:10.1029/2001JD001290.

Idone, V. P., R. E. Orville, P. Hubert, L. Barret, and A. Eybert-Berard (1984), Correlated observations of three triggered lightning flashes, *J. Geophys. Res.*, *99*(D1), 1385–1394.

Inan, U. S., J. V. Rodriguez, and V. P. Idone (1993), VLF signatures of lightning-induced heating and ionization of the nighttime *D* region, *Geophys. Res. Lett.*, *20*(21), 2355–2358, doi:10.1029/93GL02620.

Jordan, D. M., V. P. Idone, V. A. Rakov, M. A. Uman, W. H. Beasley, and H. Jurenka (1992), Observed dart leader speed in natural and triggered lightning, *J. Geophys. Res.*, *97*(D9), 9951–9957.

Karunarathne, S., T. C. Marshall, M. Stolzenburg, and N. Karunarathna (2014), Modeling initial breakdown pulses of CG lightning flashes, *Geophys. Res. Lett.*, *119*, 9003–9019, doi:10.1002/2014JD021553.

Kolmašová, I., O. Santolík, T. Farges, W. Rison, R. Lán, and L. Uhlíř (2014), Properties of the unusually short pulse sequences occurring prior to the first strokes of negative cloud-to-ground lightning flashes, *Geophys. Res. Lett.*, *41*, 5316–5324.

Kolmašová, I., O. Santolík, T. Farges, S. A. Cummer, R. Lán, and L. Uhlíř (2016), Subionospheric propagation and peak currents of preliminary breakdown pulses before negative cloud-to-ground lightning discharges, *Geophys. Res. Lett.*, *43*, 1382–1391.

Kotovsky, D. A., and R. C. Moore (2016), Photochemical response of the nighttime mesosphere to electric field heating—Recovery of electron density enhancements, *Geophys. Res. Lett.*, *43*, 952–960.

Li, J., S. Cummer, G. Lu, and L. Zigoneanu (2012), Charge moment change and lightning-driven electric fields associated with negative sprites and halos, *J. Geophys. Res.*, *117*, A09310, doi:10.1029/2012JA017731.

Marshall, T., W. Schulz, N. Karunarathna, S. Karunarathna, M. Stolzenburg, C. Vergeiner, and T. Warner (2014), On the percentage of lightning flashes that begin with initial breakdown pulses, *J. Geophys. Res. Atmos.*, *119*, 445–460, doi:10.1002/2013JD020854.

Mitchell, M. F. (2015), Very low frequency remote sensing of the lower ionosphere, PhD dissertation, Univ. Florida.

Nag, A., and V. A. Rakov (2009), Some inferences on the role of lower positive charge region in facilitating different types of lightning, *Geophys. Res. Lett.*, *36*, L05815.

Nag, A., and V. A. Rakov (2012), Positive lightning: An overview, new observations, and inferences, *J. Geophys. Res.*, *117*, D08109, doi:10.1029/2012JD017545.

Nag, A., and V. A. Rakov (2016), A unified engineering model of the first stroke in downward negative lightning, *J. Geophys. Res. Atmos.*, *121*, 2188–2204, doi:10.1002/2015JD023777.

Newsome, R. T., and U. S. Inan (2010), Free-running ground-based photometric array imaging of transient luminous events, *J. Geophys. Res.*, *115*, A00E41, doi:10.1029/2009JA014834.

Orville, R. E. (1991), Calibration of a magnetic direction finding network using measured triggered lightning return stroke peak currents, *J. Geophys. Res.*, *96*(D9), 17,135–17,142.

Pilkey, J. T. (2014), Rocket-triggered lightning propagation and North-Florida thunderstorm charge structure, PhD dissertation, Univ. of Florida.

Pilkey, J. T., M. A. Uman, J. D. Hill, T. Ngin, W. R. Gamerota, D. M. Jordan, J. Caicedo, and B. Hare (2014), Rocket-triggered lightning propagation paths relative to preceding natural lightning activity and inferred cloud charge, *J. Geophys. Res. Atmos.*, *119*, 13,427–13,456, doi:10.1002/2014JD022139.

Rakov, V. A., and M. A. Uman (2003), *Lightning Physics and Effects*, Cambridge Univ. Press, Cambridge, U. K.

Rakov, V. A., S. Mallick, A. Nag, and V. B. Somu (2014), Lightning Observatory in Gainesville (LOG), Florida: A review of recent results, *Electr. Power System. Res.*, *113*, 95–103.

Saba, M. M. F., K. L. Cummins, T. A. Warner, E. P. Krider, L. Z. S. Campos, M. G. Ballarotti, O. Pinto Jr., and S. A. Fleenor (2008), Positive leader characteristics from high-speed video observations, *Geophys. Res. Lett.*, *35*, L07802.

Said, R. K., U. S. Inan, and K. L. Cummins (2010), Long–range lightning geolocation using a VLF radio atmospheric waveform bank, *J. Geophys. Res.*, *115*, D23108, doi:10.1029/2010JD013863.

Said, R. K., M. B. Cohen, and U. S. Inan (2013), Highly intense lightning over the oceans: Estimated peak currents from global GLD360 observations, *J. Geophys. Res. Atmos.*, *118*, 6905–6915, doi:10.1002/jgrd.50508.

Salut, M. M., M. Abdullah, K. L. Graf, M. B. Cohen, B. R. T. Cotts, and S. Kumar (2012), Long recovery VLF perturbations associated with lightning discharges, *J. Geophys. Res.*, *117*, A08311, doi:10.1029/2012JA017567.

Salut, M. M., M. B. Cohen, M. A. M. Ali, K. L. Graf, B. R. T. Cotts, and S. Kumar (2013), On the relationship between lightning peak current and early VLF perturbations, *J. Geophys. Res. Space Physics*, *118*, 7272–7282, doi:10.1002/2013JA019087.

Sampath, H. T., U. S. Inan, and M. P. Johnson (2000), Recovery signatures and occurrence properties of lightning-associated subionospheric VLF perturbations, *J. Geophys. Res.*, *105*(A1), 183–191.

Schonland, B. F. J. (1937), Progressive lightning IV—The discharge mechanism, *Proc. R. Soc. London, Ser. A*, *164*(916), 132–150.

Schonland, B. F. J., D. B. Hodges, and H. Collens (1938a), Progressive lightning V—A comparison of photographic and electrical studies of the discharge process, *Proc. R. Soc. London, Ser. A*, *166*(924), 56–75.

Schonland, B. F. J., D. J. Malan, and H. Collens (1938b), Progressive lightning VI, *Proc. R. Soc. London, Ser. A*, *168*(935), 455–469.

Stolzenburg, M., T. C. Marshall, S. Karunarathna, N. Karunarathna, L. E. Vickers, T. A. Warner, R. E. Orville, and H.-D. Betz (2013), Luminosity of initial breakdown in lightning, *J. Geophys. Res. Atmos.*, *118*, 2918–2937, doi:10.1002/jgrd.50276.

Stolzenburg, M., T. C. Marshall, S. Karunarathne, N. Karunarathna, and R. E. Orville (2014), Leader observations during the initial breakdown stage of a lightning flash, *J. Geophys. Res. Atmos.*, *119*(21), 12,198–12,221, doi:10.1002/2014JD021994.

Taylor, M. J., et al. (2008), Rare measurements of a sprite with halo event driven by a negative lightning discharge over Argentina, *Geophys. Res. Lett.*, *35*, L14812, doi:10.1029/2008GL033984.

Ushio, T., Z.-I. Kawasaki, K. Matsu-ua, and D. Wang (1998), Electric fields of initial breakdown in positive ground flash, *J. Geophys. Res.*, *103*(D12), 14,135–14,139.

van der Velde, O. A., et al. (2010), Multi-instrumental observations of a positive gigantic jet produced by a winter thunderstorm in Europe, *J. Geophys. Res.*, *115*, D24301, doi:10.1029/2010JD014442.

Weidman, C. D., and E. P. Krider (1979), The radiation field wave forms produced by intracloud lightning discharge processes, *J. Geophys. Res.*, *84*(C6), 3159–3164.

Wilkes, R. A., M. A. Uman, J. T. Pilkey, and D. M. Jordan (2016), Luminosity in the initial breakdown stage of cloud-to-ground and intracloud lightning, *J. Geophys. Res. Atmos.*, *121*(3), 1236–1247, doi:10.1002/2015JD024137.

Williams, E., et al. (2012), Resolution of the sprite polarity paradox: The role of halos, *Radio Sci.*, *47*, RS2002, doi:10.1029/2011RS004794.

Wu, T., Y. Takayanagi, T. Funaki, S. Yoshida, T. Ushio, Z.-I. Kawasaki, T. Morimoto, and M. Shimizu (2013), Preliminary breakdown pulses of cloud-to-ground lightning in winter thunderstorms in Japan, *J. Atmos. Sol. Terr. Phys.*, *102*, 91–98.

Zhu, Y., V. A. Rakov, S. Mallick, and M. D. Tran (2015), Characterization of negative cloud-to-ground lightning in Florida, *J. Atmos. Sol. Terr. Phys.*, *136*, 8–15.